

# High resolution far infrared spectroscopy of IBr using a synchrotron source

By B. NELANDER<sup>1</sup>, V. SABLINSKAS<sup>2</sup>, M. DULICK<sup>3</sup>, V. BRAUN<sup>4</sup> and P. F. BERNATH<sup>4†</sup>

<sup>1</sup>Thermochemistry, Chemical Center, University of Lund, P.O. Box 124, S-22100 Lund, Sweden

<sup>2</sup>Department of General Physics and Spectroscopy, Vilnius University, Universiteto Str. 3, Vilnius, 2734 Lithuania

<sup>3</sup>National Solar Observatory, National Optical Astronomy Observatories, PO Box 26732, Tucson, AZ 85726, USA

<sup>4</sup>Department of Chemistry, University of Waterloo, Waterloo, Ontario, Canada N2L 3G1

(Received 15 July 1997; accepted 25 July 1997)

The high resolution far infrared absorption spectrum of IBr was recorded with a Fourier transform spectrometer. The fundamental 1–0 vibration–rotation band and the 2–1 and 3–2 hot bands were recorded at a resolution of  $0.00125\text{ cm}^{-1}$ . The infrared continuum was provided by synchrotron radiation emission from the Max-I storage ring. For high resolution spectroscopy at  $250\text{ cm}^{-1}$  synchrotron radiation is about 5 times brighter than a conventional infrared glower. This increase in flux at the detector resulted in a corresponding increase in the signal-to-noise ratio and a much improved infrared spectrum.

## 1. Introduction

The halogen and interhalogen molecules continue to be extensively studied species. We recently recorded a far infrared absorption spectrum of IBr [1] thus completing the spectroscopic studies of interhalogen molecules in the infrared (IF [2], ICl [3], IBr [1], BrCl [4, 5], BrF [5–7], ClF [7]). The previous IBr paper [1] reviewed the IBr spectroscopic literature prior to 1993. Since then additional papers have appeared, for example, the analyses of the  $A^3\Pi_1-X^1\Sigma^+$  system [8, 9] some vacuum ultraviolet transitions [10, 11] and a number of UV transitions connecting to the  $A^3\Pi_1$  and  $A^3\Pi_2$  states [12–14]. Even an investigation concerned with the femtosecond wavepacket dynamics in the  $B^3\Pi_0^+$  state of IBr has also been reported [15].

Shortly after our conventional far infrared spectrum of IBr was published [1] new spectra were recorded at Lund using a storage ring as the source of continuum radiation. These new spectra have an improved resolution and a higher signal-to-noise ratio because of the higher brightness achievable with such a source. The virtues of synchrotron radiation are well known for

ultraviolet and X-ray spectroscopy but are not generally appreciated for infrared work [16, 17].

A typical storage ring like Max-I in Lund is substantially brighter (photons per  $\text{cm}^2$  per steradian) than a blackbody source at 1400 K in the far infrared region. The effective source temperature of synchrotron radiation emission in the far infrared can be in excess of 10 000 K, which is even brighter than the widely used mercury arc lamp which has an effective plasma temperature of 2000 K. In addition the synchrotron radiation is emitted from nearly a point source, since the diameter of the electron beam is less than about 1 mm. Under the experimental conditions used with the Bruker IFS 120 HR Fourier transform spectrometer at a resolution of  $0.002\text{ cm}^{-1}$  at  $250\text{ cm}^{-1}$  about 5 times more signal is expected (and observed) for the Max-I storage ring than for a glower [16].

The factor of 5 improvement in brightness of the far infrared continuum translates directly into a factor of 5 improvement in the signal-to-noise ratio, all else being equal. A Fourier transform spectrometer using a conventional blackbody rather than a synchrotron will thus require a factor of 25 more time to record an equivalent spectrum, since the signal-to-noise ratio improves only with the square root of the number of scans. Early work with synchrotron radiation sources did not provide such

† Present address: Université Libre de Bruxelles, Service de Chimie Physique Moléculaire, CP 160/09, Av F. D. Roosevelt 50, B-1050 Bruxelles, Belgium.

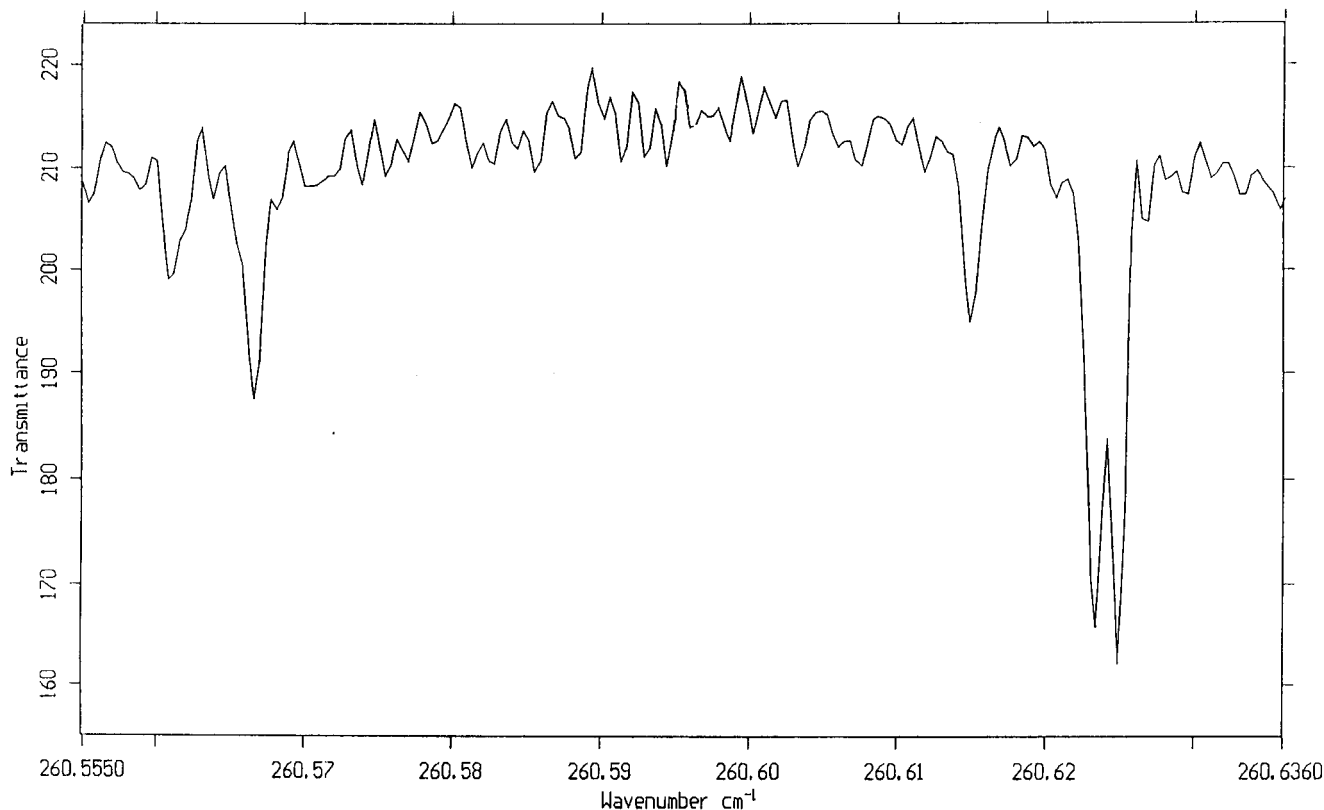


Figure 1. A portion of the infrared absorption spectrum of IBr.

dramatic improvements in far infrared performance because of electron beam motion. This random beam motion causes fluctuations in intensity at the detector and creates excess noise in the interferogram. Modern storage rings, like Max-I, however, are much more stable and the expected gain in performance is achieved in practice [16]

## 2. Experimental

The far infrared spectrum of IBr was recorded at Lund with a Bruker IFS 120 HR spectrometer and the Max-I electron storage ring. The IBr sample was contained in an evacuated 20 cm cell sealed with polyethylene windows at a total pressure of 0.6 Torr. The beam current in the Max-I storage ring was 95–140 mA and the radiation passed through a KRS-5 window before entering the spectrometer.

The Bruker spectrometer was operated with a 4 mm entrance aperture at a resolution of  $0.00125 \text{ cm}^{-1}$ . A  $6 \mu\text{m}$  mylar beamsplitter was used along with a silicon bolometer detector operated at 4.2 K. Eight scans were co-added.

The absorption lines were measured using the PC-DECOMP program developed by J. Brault and then

calibrated with residual water lines. The estimated precision of the measurements is  $\pm 0.0001 \text{ cm}^{-1}$ .

## 3. Results and discussion

A typical section of the spectrum is presented in figure 1. The resolution is improved by a factor of 2.5 and the signal-to-noise ratio by a factor of more than 3 over the previous measurements [1]. The improved signal-to-noise ratio allowed the 3–2 hot band to be measured plus the 2–1 and 1–0 bands [1]. The measured line positions are reported in table 1 for  $I^{79}\text{Br}$  and table 2 for  $I^{81}\text{Br}$ . The line assignments were made easily with the previous spectroscopic constants [1].

In reducing the data of tables 1 and 2 to spectroscopic constants, the microwave [18] and millimetre wave [19] transitions were included. The pure rotational lines were corrected for the effects of hyperfine structure, and they are provided in table 3 for convenience. These lines were included in all of our fits.

The lines of tables 1–3 were fitted using the conventional Dunham expression [20]

$$E_{vJ} = \sum Y_{ij} \left( v + \frac{1}{2} \right)^i [J(J+1)]^j, \quad (1)$$

and the constants listed in table 4. These constants are more than an order of magnitude more precise than

Table 1.  $I^{79}\text{Br}$  infrared transitions (in  $\text{cm}^{-1}$ )<sup>a</sup>.

Line	Observed	$\delta$	Line	Observed	$\delta$	Line	Observed	$\delta$	Line	Observed	$\delta$			
(1, 0) Band														
P(111)	252-081 08	26	P(108)	252-547 00	1	P(105)	253-008 71	- 105	P(104)	253-163 18	- 9			
P(103)	253-316 56	15	P(102)	253-469 12	- 4	P(101)	253-621 63	8	P(100)	253-764 13	- 942			
P(98)	254-076 21	- 21	P(97)	254-227 45	15	P(96)	254-378 03	24	P(95)	254-527 87	- 2			
P(92)	254-975 87	- 10	P(91)	255-124 39	- 18	P(90)	255-272 79	- 1	P(89)	255-420 63	- 1			
P(88)	255-568 07	- 4	P(87)	255-714 95	- 25	P(86)	255-861 88	- 3	P(85)	256-008 09	- 15			
P(72)	257-875 99	- 1	P(71)	258-017 00	- 1	P(69)	258-297 97	8	P(68)	258-437 82	6			
P(67)	258-577 30	6	P(66)	258-716 33	0	P(65)	258-855 08	2	P(64)	258-993 46	6			
P(63)	259-131 31	- 4	P(62)	259-268 91	- 1	P(61)	259-406 15	3	P(60)	259-542 85	- 7			
P(59)	259-679 30	- 4	P(58)	259-815 35	- 3	P(57)	259-951 07	2	P(56)	260-086 31	0			
P(55)	260-221 12	- 8	P(54)	260-355 70	- 1	P(53)	260-489 77	- 6	P(52)	260-623 53	- 3			
P(51)	260-756 91	- 1	P(50)	260-889 95	6	P(49)	261-022 54	6	P(48)	261-154 69	2			
P(47)	261-286 50	1	P(46)	261-417 98	7	P(45)	261-548 99	4	P(44)	261-679 59	- 1			
P(43)	261-809 96	8	P(42)	261-939 75	0	P(41)	262-069 27	1	P(40)	262-198 27	- 9			
P(39)	262-327 17	8	P(38)	262-455 40	- 2	P(37)	262-583 41	4	P(36)	262-710 92	- 1			
P(35)	262-838 15	4	P(34)	262-964 83	- 5	P(33)	263-091 29	0	P(32)	263-217 50	20			
P(31)	263-342 95	3	P(30)	263-468 22	7	P(29)	263-593 03	3	P(28)	263-717 44	0			
P(27)	263-841 54	3	P(26)	263-965 22	3	P(25)	264-088 44	- 2	P(24)	264-211 35	- 1			
P(23)	264-333 92	5	P(22)	264-456 03	4	P(21)	264-577 74	3	P(20)	264-699 12	7			
P(19)	264-820 07	8	P(18)	264-940 56	1	P(17)	265-060 63	- 7	P(16)	265-180 56	9			
P(15)	265-299 92	7	P(14)	265-418 80	- 2	P(13)	265-537 41	0	P(12)	265-655 85	23			
P(11)	265-773 47	4	P(10)	265-890 92	8	P(9)	266-007 76	- 9	P(7)	266-240 11	- 59			
P(5)	266-471 44	- 55	R(6)	267-826 53	6	R(7)	267-936 71	- 4	R(8)	268-046 64	- 1			
R(10)	268-265 22	- 3	R(11)	268-373 89	- 6	R(12)	268-482 30	3	R(13)	268-590 08	- 8			
R(14)	268-697 68	0	R(15)	268-804 56	- 21	R(16)	268-911 63	14	R(17)	269-017 81	2			
R(18)	269-123 75	5	R(19)	269-229 22	2	R(20)	269-334 30	0	R(21)	269-439 06	5			
R(22)	269-543 30	0	R(23)	269-647 24	3	R(24)	269-750 65	- 5	R(25)	269-853 78	- 1			
R(26)	269-956 69	19	R(27)	270-058 78	0	R(28)	270-160 88	21	R(29)	270-262 14	- 1			
R(30)	270-363 25	1	R(31)	270-463 93	2	R(32)	270-564 20	1	R(33)	270-664 05	0			
R(34)	270-763 52	0	R(35)	270-862 51	- 5	R(36)	270-961 23	1	R(37)	261-059 49	2			
R(38)	271-157 36	5	R(39)	271-254 75	0	R(40)	271-351 48	- 28	R(41)	271-448 47	7			
R(42)	271-544 66	5	R(43)	271-640 47	5	R(44)	271-735 86	5	R(45)	271-830 86	5			
R(46)	271-925 39	0	R(47)	272-019 59	3	R(48)	272-113 26	- 6	R(49)	272-206 71	3			
R(50)	272-299 66	3	R(51)	272-392 37	20	R(52)	272-484 32	3	R(53)	272-576 00	0			
R(54)	272-667 31	0	R(55)	272-758 42	21	R(56)	272-848 71	2	R(57)	272-938 75	0			
R(58)	273-028 44	2	R(59)	273-117 67	0	R(60)	273-206 54	4	R(61)	273-294 97	5			
R(62)	273-382 95	2	R(63)	273-470 51	- 1	R(64)	263-557 68	- 2	R(65)	273-644 47	0			
R(66)	237-730 84	1	R(67)	273-816 77	1	R(68)	273-902 43	15	R(69)	273-987 54	15			
R(70)	274-072 07	0	R(71)	274-156 43	8	R(72)	274-240 24	3	R(73)	274-323 72	7			
R(74)	274-406 72	4	R(75)	274-489 27	0	R(76)	274-571 43	- 3	R(77)	274-653 29	5			
R(78)	274-734 69	10	R(79)	274-815 46	- 5	R(80)	274-895 84	- 19	T(81)	274-976 16	3			
R(82)	275-055 83	3	R(83)	275-135 04	- 1	R(84)	275-213 95	6	R(85)	275-292 40	10			
R(86)	275-370 18	- 10	R(87)	275-447 92	6	R(88)	275-525 12	12	R(89)	275-601 72	0			
R(90)	275-678 06	3	R(91)	275-753 88	- 2	R(92)	275-829 38	2	R(93)	275-904 39	0			
R(94)	275-979 05	5	R(95)	276-053 25	7	R(96)	276-127 04	11	R(97)	276-200 24	- 3			
R(98)	276-273 27	9	R(99)	276-345 72	6	R(100)	276-417 65	- 5	R(101)	276-489 30	- 3			
R(102)	276-560 63	9	R(103)	276-631 22	- 8	R(104)	276-701 81	16	R(105)	276-771 53	- 3			
R(106)	276-840 91	- 14	R(107)	276-909 93	- 17	R(108)	276-978 65	- 8	R(109)	277-046 72	- 21			
R(110)	277-114 66	- 4	(2, 1) Band											
P(107)	251-087 18	- 17	P(104)	215-548 71	29	P(101)	252-006 17	9	P(98)	252-460 21	- 11			
P(97)	252-611 07	9	P(96)	252-761 44	18	P(92)	253-358 69	11	P(87)	254-096 50	- 17			
P(85)	254-389 14	- 10	P(81)	254-969 72	- 9	P(80)	255-113 97	- 3	P(79)	255-257 63	- 18			
P(78)	255-401 19	- 4	P(77)	255-544 45	16	P(76)	255-686 80	- 14	P(75)	255-829 29	6			

(continued)

Table 1. *Continued.*

Line	Observed	$\delta$	Line	Observed	$\delta$	Line	Observed	$\delta$	Line	Observed	$\delta$
P(74)	255-971 13	1	P(73)	256-113 22	58	P(74)	256-253 72	- 4	P(57)	258-324 60	- 7
P(56)	258-459 58	- 7	P(55)	258-594 31	5	P(54)	258-728 35	- 11	P(53)	258-862 16	- 12
P(52)	258-995 79	6	P(51)	259-128 78	0	P(50)	259-261 44	0	P(49)	259-393 78	5
P(48)	259-525 67	5	P(47)	259-657 13	1	P(46)	259-788 24	0	P(45)	259-919 05	8
P(44)	260-049 30	0	P(43)	260-179 18	- 8	P(42)	260-308 83	0	P(41)	260-437 96	- 4
P(39)	260-695 19	0	P(38)	260-823 10	- 10	P(37)	260-950 88	5	P(36)	261-078 07	1
P(35)	261-204 99	8	P(34)	261-331 11	- 24	P(33)	261-457 48	6	P(32)	261-583 09	0
P(31)	261-708 30	- 7	P(30)	261-833 17	- 9	P(29)	261-957 85	8	P(28)	262-081 96	8
P(27)	262-205 58	- 1	P(26)	262-328 95	2	P(25)	262-451 63	- 23	P(24)	262-574 47	6
P(23)	262-696 60	4	P(22)	262-818 27	- 4	P(21)	262-939 70	1	P(20)	263-060 66	0
P(19)	263-181 08	- 16	P(18)	263-301 54	10	P(17)	263-421 19	- 3	P(16)	263-540 62	- 1
P(15)	263-659 71	7	P(14)	263-778 46	20	P(13)	263-896 49	1	P(12)	264-014 30	0
P(11)	264-131 69	- 3	R(13)	266-938 38	- 10	R(14)	267-045 38	- 19	R(15)	267-152 33	7
R(16)	267-258 37	- 15	R(17)	267-364 36	- 4	R(18)	267-469 79	- 8	R(19)	267-574 95	0
R(20)	267-679 66	4	R(21)	267-783 98	9	R(22)	267-887 76	1	R(23)	267-991 13	- 7
R(24)	268-094 25	0	R(25)	268-196 85	- 5	R(26)	268-299 10	- 5	R(27)	268-401 09	9
R(28)	268-502 42	0	R(29)	268-603 47	1	R(30)	268-704 13	4	R(31)	268-804 56	25
R(32)	268-904 07	- 4	R(33)	269-003 02	- 50	R(34)	269-102 55	2	R(35)	269-201 16	4
R(36)	269-299 27	- 3	R(37)	269-397 03	- 4	R(38)	269-494 42	- 2	R(39)	269-591 37	- 4
R(40)	269-688 03	6	R(41)	269-784 11	0	R(42)	269-879 78	- 6	R(43)	269-975 18	0
R(44)	270-070 10	1	R(45)	270-155 34	- 925	R(46)	270-258 82	13	R(47)	270-352 34	- 3
R(48)	270-445 62	- 2	R(49)	270-538 53	1	R(50)	270-631 10	13	R(51)	270-723 11	10
R(52)	270-814 62	- 1	R(53)	270-905 82	- 2	R(54)	270-996 75	9	R(55)	271-086 97	- 7
R(57)	271-266 60	1	R(58)	271-355 78	5	R(59)	271-444 52	5	R(60)	271-532 74	- 4
R(61)	271-620 66	- 2	R(62)	271-708 23	5	R(63)	271-795 24	- 1	R(64)	271-881 98	7
R(65)	271-968 17	1	R(66)	272-053 94	- 3	R(67)	272-139 34	- 4	R(68)	272-224 49	11
R(69)	272-308 71	- 23	R(70)	272-392 37	- 73	R(71)	272-476 99	15	R(72)	272-560 20	4
R(73)	272-643 15	9	R(74)	272-725 48	- 5	R(75)	272-807 89	29	R(76)	272-889 30	6
R(77)	272-970 68	22	R(78)	273-051 45	19	R(79)	273-131 78	14	R(80)	273-211 52	- 7
R(81)	273-291 29	16	R(87)	273-759 62	15	R(88)	273-836 05	1	R(91)	274-063 36	15
(3, 2) Band											
P(78)	253-773 62	146	P(66)	255-460 29	3	P(63)	255-873 36	- 25	P(62)	256-010 58	- 4
P(53)	257-226 08	- 23	P(52)	257-359 35	- 10	P(44)	258-410 51	- 5	P(43)	258-540 22	1
P(42)	258-669 18	- 26	P(41)	258-798 27	- 3	P(31)	260-065 40	3	P(30)	260-190 31	39
P(29)	260-314 31	26	P(27)	260-561 41	19	P(26)	260-683 99	- 20	P(25)	260-807 09	31
P(24)	260-928 69	- 27	P(23)	261-050 76	0	P(22)	261-172 33	16	P(18)	261-653 63	- 20
P(15)	262-010 83	- 11	P(14)	262-129 05	- 13	R(25)	266-531 56	12	R(26)	266-633 44	20
R(27)	266-734 52	- 10	R(28)	266-835 64	3	R(26)	266-936 25	6	R(31)	267-136 25	14
R(33)	267-335 40	99	R(36)	267-628 80	1	R(37)	267-726 01	- 8	R(38)	267-823 13	14
R(39)	267-919 59	11	R(40)	268-015 64	8	R(44)	268-395 67	- 7	R(48)	268-769 59	23
R(51)	269-045 28	5	R(52)	269-136 19	- 15	R(53)	269-227 26	19	R(54)	269-317 29	- 7
R(65)	270-282 93	- 24	R(67)	270-453 58	22	R(68)	270-538 53	72			

<sup>a</sup> Observed - calculated differences (columns labelled  $\delta$ ) are in units of  $0.000\,01\text{ cm}^{-1}$ .

those reported in [1] and comparable with those of [8]. Appadoo *et al.* [8] used the new vibration-rotation lines reported here in a much more extensive fit of the  $A^3\Pi_1-X^1\Sigma^+$  transition.

The  $I^{79}\text{Br}$  and  $I^{81}\text{Br}$  lines can be fitted together using the mass-independent Dunham expression [21, 22]

$$E_{v,J} = \sum_{\mu} \frac{U_{ij}}{i!2^j} (v + \frac{1}{2})^i [J(J+1)]^j. \quad (2)$$

The mass dependence of the  $Y_{ij}$  constants has been factored out explicitly in equation (2), assuming the Born-Oppenheimer approximation. In our new com-

Table 2.  $I^{81}\text{Br}$  infrared transitions (in  $\text{cm}^{-1}$ )<sup>a</sup>.

Line	Observed	$\delta$	Line	Observed	$\delta$	Line	Observed	$\delta$	Line	Observed	$\delta$
(1, 0) Band											
P(111)	250-297 90	- 4	P(110)	250-451 03	0	P(108)	250-756 00	- 8	P(107)	250-908 24	17
P(106)	251-059 74	5	P(105)	251-210 98	5	P(104)	251-361 95	14	P(103)	251-512 20	- 11
P(102)	251-662 49	3	P(101)	251-811 91	- 31	P(100)	251-961 61	- 1	P(99)	252-110 80	13
P(98)	252-259 31	- 1	P(97)	252-407 76	13	P(96)	252-555 57	1	P(95)	252-703 04	- 7
P(94)	252-850 12	- 18	P(93)	252-996 96	- 16	P(92)	253-143 47	- 10	P(91)	253-289 67	1
P(90)	253-435 27	- 9	P(89)	253-580 94	22	P(88)	253-725 81	11	P(87)	253-870 34	4
P(86)	254-014 38	- 14	P(85)	254-158 34	- 4	P(84)	254-301 98	9	P(82)	254-587 64	- 10
P(81)	254-730 13	0	P(80)	254-871 96	- 17	P(79)	255-013 57	- 20	P(78)	255-155 15	11
P(77)	255-295 95	2	P(76)	255-436 38	- 6	P(75)	255-576 64	4	P(74)	255-716 49	11
P(73)	255-855 77	- 1	P(72)	255-994 80	- 1	P(71)	256-133 12	- 35	P(70)	256-272 16	39
P(63)	257-229 05	- 27	P(62)	257-364 77	14	P(58)	257-902 14	5	P(57)	258-035 44	- 7
P(56)	258-168 16	- 40	P(55)	258-301 22	- 2	P(54)	258-433 55	0	P(53)	258-565 46	- 1
P(52)	258-697 10	7	P(51)	258-828 23	3	P(50)	258-959 01	1	P(49)	259-089 40	- 2
P(48)	259-219 50	3	P(47)	259-349 09	- 4	P(46)	259-478 41	- 2	P(45)	259-607 29	- 5
P(44)	259-735 89	0	P(43)	259-864 04	0	P(42)	259-991 86	2	P(41)	260-119 13	- 10
P(40)	260-246 20	- 6	P(39)	260-373 03	11	P(38)	260-499 16	- 2	P(37)	260-615 23	- 985
P(36)	260-750 60	0	P(35)	260-875 77	3	P(34)	261-000 51	1	P(33)	261-124 91	4
P(32)	261-248 85	- 1	P(31)	261-372 45	- 3	P(30)	261-495 76	3	P(29)	261-618 60	1
P(28)	261-741 06	0	P(27)	261-863 15	0	P(26)	261-984 87	0	P(25)	262-106 18	- 3
P(24)	262-227 09	- 7	P(23)	262-347 73	- 1	P(22)	262-468 00	6	P(21)	262-587 79	4
P(20)	262-707 20	2	P(19)	262-826 10	- 11	P(18)	262-944 93	4	P(17)	263-063 19	2
P(15)	263-298 58	0	P(14)	263-415 80	9	P(13)	263-532 45	0	P(12)	263-648 84	2
P(11)	263-764 92	12	P(10)	263-880 26	- 13	P(9)	263-995 65	4	P(8)	264-110 50	6
R(6)	265-786 22	- 32	R(7)	265-895 09	- 9	R(8)	266-003 41	- 2	R(9)	266-111 20	- 9
R(11)	266-326 01	15	R(12)	266-432 47	- 8	R(13)	266-538 88	2	R(14)	266-644 75	- 2
R(15)	266-750 57	27	R(16)	266-855 43	0	R(17)	266-960 15	- 2	R(18)	267-064 48	- 4
R(19)	267-168 47	- 1	R(20)	267-272 08	2	R(21)	267-375 27	3	R(22)	267-478 01	- 1
R(23)	267-580 53	11	R(24)	267-682 43	1	R(26)	267-885 25	1	R(27)	267-986 07	1
R(29)	268-186 06	- 44	R(30)	268-286 14	0	R(31)	268-385 36	- 2	R(32)	268-484 25	1
R(33)	268-582 82	13	R(34)	268-680 71	- 3	R(35)	268-778 37	- 3	R(36)	268-875 76	8
R(37)	268-972 59	4	R(38)	269-069 00	- 1	R(39)	269-165 10	1	R(40)	269-260 75	- 1
R(41)	269-355 71	- 33	R(42)	269-450 89	- 4	R(43)	269-545 46	4	R(44)	269-639 46	- 4
R(45)	269-733 17	- 1	R(46)	269-826 48	0	R(47)	269-919 35	- 1	R(48)	270-011 80	- 5
R(49)	270-103 94	- 1	R(50)	270-195 65	0	R(51)	270-286 96	2	R(52)	270-377 82	0
R(53)	270-468 33	1	R(54)	270-558 38	- 1	R(55)	270-648 13	4	R(56)	270-737 38	1
R(57)	270-826 27	2	R(58)	270-914 65	- 7	R(60)	271-090 51	3	R(61)	271-177 52	- 22
R(62)	271-264 55	- 6	R(64)	271-437 07	- 6	R(65)	271-522 80	0	R(66)	271-608 02	- 1
R(67)	271-692 84	- 4	R(68)	271-777 32	0	R(69)	271-861 31	- 4	R(70)	271-944 98	0
R(71)	272-028 17	- 2	R(72)	272-110 94	- 6	R(73)	272-193 33	- 8	R(74)	272-275 40	- 1
R(75)	272-357 09	8	R(76)	272-438 16	- 2	R(77)	272-518 95	0	R(78)	272-599 39	7
R(79)	272-679 34	6	R(81)	272-838 02	6	R(82)	272-916 57	- 10	R(83)	272-995 06	6
R(84)	273-072 91	1	R(85)	273-150 32	- 7	R(86)	273-227 35	- 12	R(87)	273-304 06	- 8
R(88)	273-380 44	4	R(89)	273-456 28	3	R(90)	273-531 52	- 15	R(61)	273-606 70	0
R(92)	273-682 08	78	R(93)	273-755 44	- 4	R(94)	273-829 18	- 8	R(96)	273-975 60	2
R(97)	274-048 12	1	R(99)	274-191 92	0	R(100)	274-263 21	0			
(2, 1) Band											
P(98)	250-667 95	17	P(97)	250-815 91	4	P(95)	251-111 08	14	P(93)	251-404 51	0
P(92)	251-550 78	3	P(90)	251-841 86	- 23	P(89)	251-987 21	0	P(88)	252-132 06	9
P(87)	252-276 39	5	P(96)	252-420 39	5	P(85)	252-564 25	28	P(82)	252-992 61	- 1
P(81)	253-134 64	- 12	P(80)	253-276 48	- 4	P(79)	253-417 93	0	P(78)	253-558 92	- 2
P(77)	253-699 62	2	P(74)	254-119 39	9	P(73)	254-258 53	8	P(72)	254-397 30	7
P(71)	254-535 36	- 26	P(70)	254-673 91	25	P(69)	254-811 27	- 4	P(68)	254-948 50	- 8
P(67)	255-085 40	- 9	P(66)	255-222 06	3	P(65)	255-358 19	1	P(64)	255-493 75	- 20

(continued)

Table 2. *Continued.*

Line	Observed	$\delta$	Line	Observed	$\delta$	Line	Observed	$\delta$	Line	Observed	$\delta$
P(63)	255-629 29	- 6	P(62)	255-764 58	19	P(61)	255-899 07	3	P(60)	256-033 44	13
P(45)	258-002 16	0	P(43)	258-258 41	15	P(42)	258-385 93	20	P(41)	258-512 65	- 17
P(40)	258-639 51	- 2	P(39)	258-765 86	0	P(38)	258-891 72	- 10	P(37)	259-017 37	- 2
P(36)	259-142 50	- 9	P(35)	259-267 43	2	P(34)	259-391 83	0	P(33)	259-515 81	- 7
P(32)	259-639 44	- 11	P(31)	259-762 83	- 1	P(30)	259-885 64	- 11	P(29)	260-008 14	- 13
P(28)	260-130 39	- 2	P(27)	260-252 13	- 4	P(25)	260-494 45	- 10	P(24)	260-615 49	32
P(23)	260-735 45	5	P(22)	260-855 12	- 11	P(21)	260-974 68	- 1	P(20)	261-093 82	4
P(19)	261-212 56	8	P(17)	261-448 56	- 14	P(16)	261-566 10	- 14	P(15)	261-683 45	4
P(14)	261-800 20	2	P(13)	261-916 53	- 2	P(12)	262-032 44	- 11	P(11)	262-147 99	- 18
P(8)	262-492 56	- 13	R(9)	264-486 60	6	R(10)	264-593 56	- 4	R(13)	264-912 20	- 27
R(14)	265-018 28	30	R(15)	265-123 07	- 1	R(16)	265-227 84	4	R(17)	265-331 91	- 20
R(18)	265-435 99	- 6	R(19)	265-539 40	- 18	R(20)	265-642 61	- 12	R(21)	265-745 57	8
R(22)	265-847 79	- 4	R(23)	265-949 72	- 7	R(24)	266-051 47	10	R(25)	266-152 46	- 7
R(26)	266-253 33	1	R(27)	266-353 52	- 17	R(28)	266-453 68	0	R(29)	266-553 40	13
R(30)	266-652 46	0	R(31)	266-751 51	25	R(32)	266-849 63	- 2	R(33)	266-947 68	2
R(34)	267-045 38	11	R(35)	267-142 45	- 2	R(36)	267-239 30	1	R(38)	267-431 85	14
R(39)	267-527 32	0	R(40)	267-622 57	3	R(41)	267-717 27	- 8	R(42)	267-811 76	0
R(43)	267-905 83	4	R(44)	267-999 48	8	R(45)	268-092 68	6	R(47)	268-277 91	6
R(48)	268-369 82	- 3	R(49)	268-461 44	- 2	R(50)	268-552 68	0	R(51)	268-643 44	- 3
R(52)	268-733 88	0	R(53)	268-823 92	3	R(54)	268-913 50	2	R(56)	269-091 48	1
R(57)	269-179 88	3	R(58)	269-267 80	- 3	R(59)	269-355 71	30	R(60)	269-442 59	1
R(61)	269-529 36	1	R(62)	269-615 69	- 1	R(63)	269-701 70	3	R(64)	269-787 25	4
R(65)	269-872 45	9	R(67)	270-041 45	3	R(68)	270-125 46	12	R(70)	270-291 93	- 1
R(71)	270-374 59	- 5	R(72)	270-456 94	0	R(78)	270-941 99	- 5	R(79)	271-021 35	- 10
R(80)	271-100 49	2	R(81)	271-179 26	20	R(88)	271-717 68	5			
(3, 2) Band											
P(84)	251-104 62	21	P(81)	251-531 28	5	P(75)	252-374 53	- 21	P(74)	252-513 95	- 6
P(73)	252-652 69	- 21	P(72)	252-791 18	- 24	P(68)	253-341 42	- 32	P(64)	253-886 16	12
P(58)	254-691 33	18	P(54)	255-220 19	- 11	P(53)	255-351 52	- 13	P(48)	256-002 67	0
P(29)	258-389 78	9	R(19)	263-902 36	5	R(20)	264-004 94	- 7	R(21)	264-107 36	1
R(26)	264-613 12	12	R(27)	264-712 97	3	R(31)	265-108 95	21	R(32)	265-206 79	10
R(34)	265-401 24	- 14	R(36)	265-594 58	9	R(37)	265-690 34	- 10	R(39)	265-881 07	- 7
R(40)	265-975 74	- 15	R(42)	266-164 36	17	R(43)	266-257 61	- 12	R(44)	266-350 94	6
R(45)	266-443 72	10	R(46)	266-535 85	- 10	R(47)	266-627 91	1	R(48)	266-719 40	- 2
R(51)	266-991 99	39	R(52)	267-081 42	- 9	R(54)	267-260 08	- 4	R(55)	267-348 89	6
R(57)	267-524 99	- 1	R(58)	267-612 44	- 4	R(59)	267-699 68	11	R(61)	267-872 39	- 10
R(63)	268-043 56	- 23	R(68)	268-464 84	- 4	R(70)	268-630 39	- 6	R(76)	269-117 36	6

<sup>a</sup> Observed - calculated differences (columns labelled  $\delta$ ) are in units of  $0.000\,01\text{ cm}^{-1}$ .

bined fits no evidence for Born–Oppenheimer breakdown could be detected.

The higher order  $U_{ij}$  ( $j > 1$ ) are not independent constants but can be determined using relationships such as

$$U_{02} = -\frac{4U_{01}^3}{U_{10}^2}, \quad (3)$$

that are implicit in the Dunham analysis [20–22]. We have, therefore, fitted the data of tables 1–3 using equation (2) and these relationships to obtain a set of ‘constrained’  $U_{ij}$  parameters [23]. In this way the data set

(tables 1–3) could be reproduced by only 5 independent  $U_{ij}$  parameters (table 5) compared with the 18 conventional Dunham  $Y_{ij}$ ’s (table 4).

An equally compact representation of the data was obtained by fitting the data directly to the eigenvalues of the radial Schrödinger equation. In this case a modified Morse potential,

$$U(z) = D_e \left[ \frac{1 - e^{-\beta(z)}}{1 - e^{-\beta(\infty)}} \right]^2,$$

with

Table 3. Iodine bromide  $J \rightarrow J + 1$  pure rotational transitions (in  $\text{cm}^{-1}$ ).<sup>a</sup>

$\nu$	$J$	Observed	$\delta$	$\nu$	$J$	Observed	$\delta$	$\nu$	$J$	Observed	$\delta$	$\nu$	$J$	Observed	$\delta$
$\text{I}^{79}\text{Br}$															
0	2	0.340 402 67	- 28	1	2	0.339 215 69	0	2	2	0.338 023 13	36	0	43	4.989 117	0
0	52	6.007 731	1	0	61	7.025 289	- 1	0	78	8.943 843	1	0	79	9.056 535	0
0	87	9.957 351	- 1	0	95	10.856 779	- 4	1	43	4.971 688	0	1	52	5.986 726	- 1
1	61	7.000 707	0	1	79	9.024 774	0	2	52	5.965 622	1	2	61	6.976 004	- 1
3	61	6.951 181	- 4	4	61	6.926 234	- 12								
$\text{I}^{81}\text{Br}$															
0	2	0.335 224 97	- 11	0	2	0.334 064 87	0	0	2	0.332 898 90	- 28	0	44	5.024 787	0
0	53	6.027 840	0	0	62	7.029 852	0	0	71	8.030 651	- 1	0	80	9.030 063	1
1	44	5.007 367	1	1	53	6.006 926	0	1	62	7.005 441	0	1	71	8.002 738	2
2	44	4.989 864	1	2	53	5.985 914	1	2	62	6.980 912	- 1	2	71	7.974 687	1
3	53	5.964 800	0	4	53	5.943 575	- 12	5	62	6.906 597	- 30				

<sup>a</sup> Observed - calculated differences (columns labelled  $\delta$ ) are in units of  $10^{-8} \text{cm}^{-1}$  for microwave lines and  $10^{-6} \text{cm}^{-1}$  for millimetre wave lines.

Table 4. Mass-dependent Dunham constants (in  $\text{cm}^{-1}$ ).

	$\text{I}^{79}\text{Br}$	$\text{I}^{81}\text{Br}$
$Y_{10}$	268.681 076(37)	266.627 934(37)
$Y_{20}$	- 0.816 597 6(216)	- 0.804 123 4(210)
$10^3 Y_{30}$	- 1.415 00(375)	- 1.390 99(361)
$10^2 Y_{01}$	5.683 255 33(103)	5.596 734 74(119)
$10^4 Y_{11}$	- 1.969 037 4(650)	- 1.924 291 3(653)
$10^7 Y_{21}$	- 4.787 3(140)	- 4.641 2(122)
$10^8 Y_{02}$	- 1.016 446(222)	- 0.986 162(275)
$10^{11} Y_{12}$	- 5.081 3(425)	- 4.817 3(459)
$10^{15} Y_{03}$	- 1.678(166)	- 1.314(217)

Table 5. Mass-independent Dunham constants (in  $\text{cm}^{-1}$ ).

$U_{10}$	1 874.207 68(18)	$10^8 U_{22}$	- 9.695 207 12
$U_{20}$	- 39.733 494(738)	$10^{10} U_{03}$	- 1.531 544 01
$U_{30}$	- 0.482 374(899)	$10^{11} U_{13}$	- 4.398 879 05
$U_{01}$	2.765 405 45(10)	$10^{15} U_{04}$	- 5.335 113 31
$10^2 U_{11}$	- 6.684 324 4(893)	$10^{15} U_{14}$	- 2.303 536 36
$10^3 U_{21}$	1.117 32(204)	$10^{19} U_{05}$	- 2.231 700 26
$10^5 U_{02}$	- 2.408 246 90	$10^{23} U_{06}$	- 1.042 350 62
$10^7 U_{12}$	- 7.765 773 86		

$$z = \frac{R - R_e}{R + R_e},$$

$$\beta(z) = z \sum_{i=0}^{\infty} \beta_i z^i,$$

and

$$\beta(\infty) = \sum_{i=0}^{\infty} \beta_i,$$

was used [23]. The potential parameters obtained in this way are reported in table 6. The dissociation energy was fixed to the value quoted by Huber and Herzberg [24]

Table 6. Derived parameter values for the modified Morse potential.

$D_e / \text{cm}^{-1}$	14 660.0
$R_e / \text{Å}$	2.468 985 985 7(437)
$\beta_0$	9.308 343 015(796)
$\beta_1$	17.902 504(250)
$\beta_2$	52.819 95(218)
$\beta_3$	137.052(312)
$\beta_4$	244.33(190)
$M(\text{I}) / \text{u}$	126.904 473
$M(^{79}\text{Br}) / \text{u}$	78.918 336 1
$M(^{81}\text{Br}) / \text{u}$	80.916 289

and the masses taken from Mills *et al.* [25]. This fit required 5 potential parameters ( $\beta_0$ - $\beta_4$ ) and also led to a new value for  $R_e$ , the equilibrium bond length. The utility of far infrared synchrotron radiation for high resolution absorption spectroscopy is illustrated clearly by our improved line positions and spectroscopic constants.

This work was supported by the National Sciences and Engineering Research Council of Canada (NSERC). Partial support was also provided by the Petroleum Research Fund, administered by the American Chemical Society. The infrared beam line was financed by grants from Knut and Alice Wallenbergs Stiftelse and Forskningsrådsnämnden. The stay of V.S. in Lund was supported by a stipend from the Swedish Institute.

## References

- [1] CAMPBELL, J. M., and BERNATH, P. F., 1993, *J. molec. Spectrosc.*, **158**, 339.

- [2] FRUM, C. I., ENGLEMAN, R., and BERNATH, P. F., 1990, *Chem. Phys. Lett.*, **167**, 356.
- [3] HEDDERICH, H. G., BERNATH, P. F., and McRAE, G. A., 1992, *J. molec. Spectrosc.*, **155**, 384.
- [4] UEHARA, H., KONNO, T., OZAKI, Y., HORAI, K., NAKAGAWA, K., and JOHNS, J. W. C., 1994, *Can. J. Phys.*, **72**, 1145.
- [5] NAKAGAWA, K., HORAI, K., KONNO, T., and UEHARA, H., 1988, *J. molec. Spectrosc.*, **131**, 233.
- [6] BIRK, H., 1993, *Z. Naturf.*, **48a**, 581.
- [7] BÜRGER, H., SCHULTZ, P., JACOB, E., and FÄHNLE, M., 1986, *Z. Naturf.*, **41a**, 1015.
- [8] APPADOO, D. R. T., BERNATH, P. F., and LeROY, R. J., 1994, *Can. J. Phys.*, **72**, 1265.
- [9] NISHIMIYA, N., YUKIYA, T., and SUZUKI, M., 1995, *J. molec. Spectrosc.*, **173**, 8.
- [10] YENCHA, A. J., RIDLEY, T., MAIER, R., FLOOD, R. V., LAWLEY, K. P., DONOVAN, R. J., and HOPKIRK, A., 1993, *J. phys. Chem.*, **97**, 4582.
- [11] KVARAN, A., WANG, H., and JOHANNESSON, G. H., 1995, *J. phys. Chem.*, **99**, 4451.
- [12] CLEVEGER, J. O., RAY, Q. P., TELLINGHUISEN, J., ZHENG, X., and HEAVEN, M. C., 1994, *Can. J. Phys.*, **72**, 1294.
- [13] ZHENG, X., HEAVEN, M. C., and TELLINGHUISEN, J., 1994, *J. molec. Spectrosc.*, **164**, 135.
- [14] RADZYKEWYCZ, D. T., LITTLEJOHN, C. D., CARTER, M. B., CLEVINGER, J. O., PURVIS, J. H., and TELLINGHUISEN, J., 1994, *J. molec. Spectrosc.*, **166**, 287.
- [15] VRACKING, M. J. J., VILLENEUVE, D. M., and STOLOW, A., 1996, *J. chem. Phys.*, **105**, 5647.
- [16] NELANDER, B., 1995, *Vib. Spectrosc.*, **9**, 29.
- [17] DUNCAN, W. D., and WILLIAMS, G. P., 1993, *Appl. Optics*, **22**, 2914.
- [18] TIEMANN, E., and MÖLLER, TH., 1975, *Z. Naturf.*, **30a**, 986.
- [19] WILLIS, R. E., and CLARK, W. C., 1980, *J. chem. Phys.*, **72**, 4946; R. E. Willis, 1979, Ph.D. thesis, Duke University.
- [20] DUNHAM, J. L., 1932, *Phys. Rev.*, **41**, 721.
- [21] WATSON, J. K. G., 1973, *J. molec. Spectrosc.*, **45**, 99.
- [22] WATSON, J. K. G., 1980, *J. molec. Spectrosc.*, **80**, 411.
- [23] HEDDERICH, H. G., DULICK, M., and BERNATH, P. F., 1993, *J. chem. Phys.*, **99**, 8363.
- [24] HUBER, K. P., and HERZBERG, G., 1979, *Constants of Diatomic Molecules* (New York: Van Nostrand-Reinhold).
- [25] MILLS, I. *et al.*, 1989, *IUPAC Quantities, Units and Symbols in Physical Chemistry* (Oxford: Blackwell).